SUPPORT INFORMATION

Multi-Dimensional Architecture of Ag/α-Ag2WO4 Crystals: Insights into Microstructural, Morphology, and Photoluminescent Properties

Lílian Cruz,*[a] Mayara M. Teixeira,[a] Vinícius Teodoro,[a] Natalia Jacomaci,[b] Letícia O. Laier,[b] Marcelo Assis,[a] Nadia G. Macedo,[c] Ana C. M. Tello,[a] Luís F. da Silva,[d] Gilmar E. Marques,[d] Maria A. Zaghete,[b] Márcio D. Teodoro[d] and Elson Longo *[a]

[a]Center of Development of Functional Materials, Federal University of São Carlos, Rod. Washington Luiz, km 235, 13565-905, São Carlos, SP, Brazil.

[b]Interdisciplinary laboratory of ceramic studies, São Paulo State University, 14800-900, Araraquara, SP, Brazil.

[c]Department of Physical Chemistry, Institute of Chemistry, State University of Campinas, 13083-970, Campinas, SP, Brazil.

[d]Department of Physics, Federal University of São Carlos, Rod. Washington Luiz, km 235, 13565-905, São Carlos, SP, Brazil.

Fig. S1 shows the results by the Rietveld method and **Table. S1** corroborates the statistical parameters that guarantee the quality of the refinement (GOF, R_{Bragg}, R_{exp}, R_{wp}), which have few deviations, suggesting that the refinement of the structure and the numerical results are reliable.

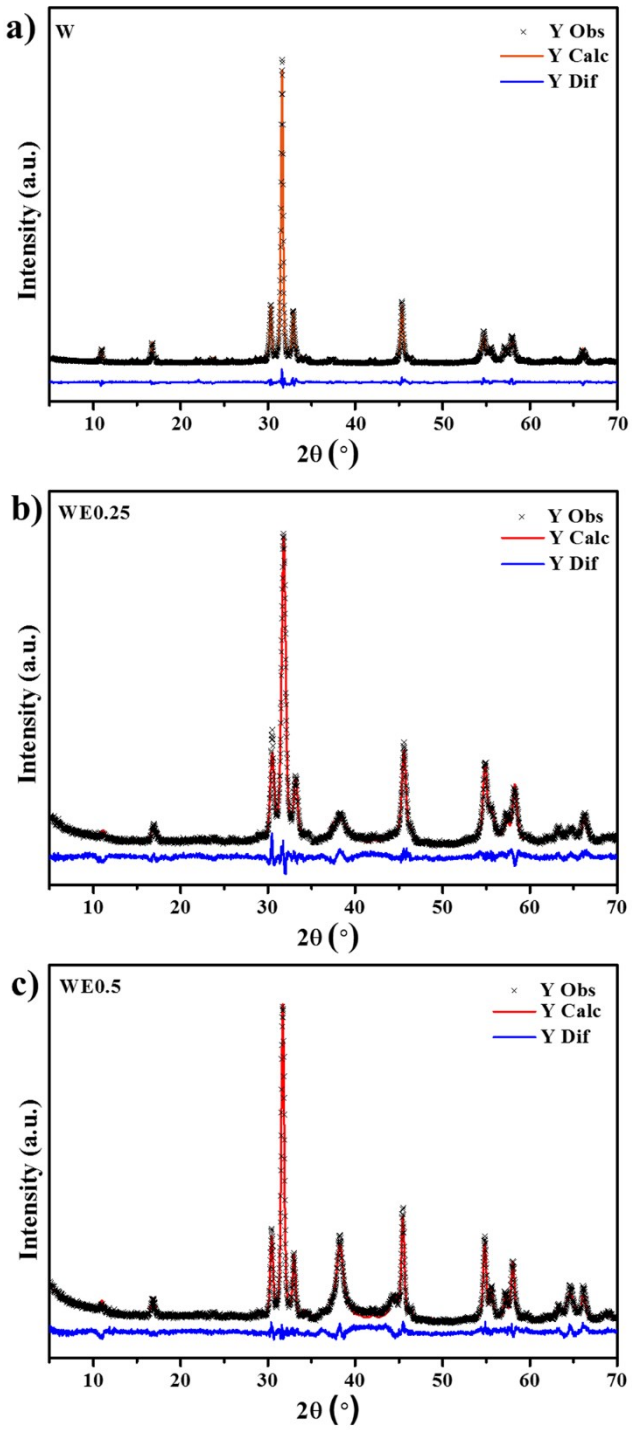

Figure S1. Rietveld refinement plot of α-Ag_2WO_4 samples prepared by the MAH method: a) W, b) WE0.25 and c) WE0.5.

Table S1. Statistical parameters obtained by Rietveld refinement of the Ag/α-Ag_2WO_4 samples.

	α-Ag_2WO_4				Ag^0
Samples	**GOF**	**R_{BRAGG}**	**R_{EXP}**	**R_{WP}**	**R_{BRAGG}**
W	**2.13**	**2.22**	**3.44**	**7.34**	*****
WE0.25	**1.66**	**2.18**	**4.83**	**7.99**	**1.29**
WE0.5	**1.81**	**3.05**	**4.86**	**8.80**	**1.10**

Deviations at the binding angle of the O-Ag-O and O-W-O can be confirmed in **Tabs. S2** and **S3**.

Table S2. Bond angles of [AgO_y] (Card ICSD n^0. 4165)[1, 2, 3].

	Ref	**W**	**WE0.25**	**WE0.5**	**|Ref-W|**	**|Ref-WE0.25|**	**|Ref-WE0.5|**
O6Ag3O6	**174.6**	**174.6**	**174.6**	**174.6**	**0.02**	**0.01**	**0.01**
O6Ag3O2	**67.6**	**67.8**	**67.7**	**67.9**	**0.20**	**0.09**	**0.26**
O6Ag3O2	**115.2**	**115.1**	**115.2**	**115.0**	**0.12**	**0.01**	**0.18**
O6Ag3O1	**66.1**	**66.3**	**66.1**	**66.3**	**0.16**	**0.04**	**0.21**
O6Ag3O1	**110.7**	**110.6**	**110.7**	**110.5**	**0.12**	**0.02**	**0.18**
O1Ag3O2	**62.4**	**62.4**	**62.5**	**62.5**	**0.06**	**0.17**	**0.10**
O2Ag3O2	**121.4**	**121.3**	**121.2**	**121.3**	**0.06**	**0.17**	**0.11**
O1Ag3O1	**113.9**	**113.9**	**113.7**	**113.8**	**0.05**	**0.16**	**0.09**
O4Ag4O7	**94.7**	**94.6**	**94.7**	**94.6**	**0.13**	**0.01**	**0.16**

O4Ag4O4	**110.7**	**110.6**	**110.5**	**110.5**	**0.13**	**0.22**	**0.19**
O4Ag4O7	**99.5**	**99.6**	**99.5**	**99.6**	**0.10**	**0.03**	**0.15**
O7Ag4O7	**154.9**	**155.0**	**154.9**	**155.0**	**0.07**	**0.02**	**0.06**
O3Ag5O8	**89.9**	**89.8**	**89.9**	**89.8**	**0.12**	**0.02**	**0.15**
O3Ag5O8	**106.4**	**106.6**	**106.5**	**106.6**	**0.13**	**0.07**	**0.18**
O3Ag5O3	**130.1**	**130.0**	**129.9**	**130.0**	**0.09**	**0.16**	**0.14**
O8Ag5O8	**141.0**	**141.1**	**140.9**	**141.1**	**0.08**	**0.06**	**0.07**
O5Ag6O5	**170.4**	**170.4**	**170.4**	**170.4**	**0.04**	**0.01**	**0.03**
O1Ag1O2	**139.0**	**139.0**	**139.0**	**139.0**	**0.04**	**0.00**	**0.04**
O1Ag1O3	**104.4**	**104.2**	**104.3**	**104.1**	**0.23**	**0.06**	**0.29**
O1Ag1O4	**97.3**	**97.5**	**97.4**	**97.6**	**0.22**	**0.11**	**0.28**
O1Ag1O5	**63.8**	**64.0**	**63.8**	**64.0**	**0.15**	**0.03**	**0.18**
O1Ag1O7	**141.0**	**141.0**	**140.9**	**140.9**	**0.04**	**0.08**	**0.07**
O1Ag1O8	**87.7**	**87.8**	**87.9**	**87.8**	**0.08**	**0.15**	**0.10**
O1Ag2O2	**140.6**	**140.6**	**140.6**	**140.6**	**0. 13**	**0.02**	**0.02**
O1Ag2O3	**57.9**	**57.8**	**57.9**	**57.8**	**0.07**	**0.02**	**0.11**
O1Ag2O4	**83.0**	**83.1**	**82.9**	**83.1**	**0.08**	**0.07**	**0.10**
O1Ag2O5	**127.1**	**127.1**	**127.2**	**127.0**	**0.05**	**0.12**	**0.06**
O1Ag2O7	**57.7**	**57.6**	**57.5**	**57.6**	**0.08**	**0.20**	**0.12**
O1Ag2O8	**76.3**	**76.4**	**76.4**	**76.4**	**0.05**	**0.13**	**0.09**

Table S3. Bond angles of [WO_6] (Card ICSD n^0. 4165)[1, 2, 3].

	Ref	W	WE0.25	WE0.5	|Ref-W|	|Ref-WE0.25|	|Ref-WE0.5|
O8W1O7	**106.2**	**106.2**	**106.3**	**106.3**	**0.01**	**0.10**	**0.04**
O8W1O5	**99.3**	**99.1**	**99.2**	**99.1**	**0.18**	**0.12**	**0.23**
O8W1O2	**80.1**	**80.1**	**79.9**	**80.1**	**0.03**	**0.18**	**0.07**
O8W1O6	**93.1**	**93.3**	**93.2**	**93.3**	**0.13**	**0.03**	**0.16**
O8W1O1	**159.3**	**159.3**	**159.4**	**159.3**	**0.02**	**0.01**	**0.02**
O7W1O5	**109.2**	**109.1**	**109.17**	**109.0**	**0.14**	**0.06**	**0.19**
O5W1O2	**84.8**	**85.0**	**84.9**	**85.0**	**0.15**	**0.03**	**0.19**
O2W1O6	**71.4**	**71.2**	**71.4**	**71.2**	**0.19**	**0.06**	**0.23**
O6W1O7	**92.2**	**92.3**	**92.3**	**92.4**	**0.12**	**0.02**	**0.16**
O1W1O7	**90.2**	**90.1**	**90.0**	**90.07**	**0.04**	**0.18**	**0.09**
O1W1O5	**86.8**	**87.0**	**86.9**	**87.0**	**0.16**	**0.05**	**0.21**
O1W1O2	**80.8**	**80.8**	**81.0**	**80.8**	**0.02**	**0.15**	**0.01**
O1W1O6	**73.2**	**73.1**	**73.2**	**73.0**	**0.15**	**0.00**	**0.19**
O6W2O4	**158.8**	**158.8**	**158.8**	**158.8**	**0.02**	**0.01**	**0.02**
O6W2O4	**89.1**	**89.1**	**89.2**	**89.2**	**0.06**	**0.18**	**0.10**
O6W2O2	**76.0**	**75.8**	**75.9**	**75.8**	**0.14**	**0.06**	**0.18**
O6W2O6	**72.2**	**72.2**	**72.0**	**72.1**	**0.04**	**0.18**	**0.07**
O6W2O2	**85.6**	**85.7**	**85.5**	**85.7**	**0.12**	**0.02**	**0.15**
O2W2O4	**99.9**	**99.7**	**99.8**	**99.6**	**0.17**	**0.013**	**0.22**
O4W2O2	**93.0**	**93.2**	**93.1**	**93.3**	**0.18**	**0.08**	**0.24**
O4W2O4	**111.0**	**110.9**	**110.8**	**110.8**	**0.08**	**0.19**	**0.13**

O3W3O6	**166.1**	**166.1**	**166.1**	**166.2**	**0.01**	**0.00**	**0.01**
O3W3O1	**96.2**	**96.4**	**96.1**	**96.4**	**0.14**	**0.17**	**0.20**
O3W3O3	**100.7**	**100.6**	**100.4**	**100.5**	**0.08**	**0.21**	**0.13**
O3W3O1	**96.1**	**95.9**	**96.3**	**96.0**	**0.22**	**0.13**	**0.27**
O3W3O6	**92.6**	**92.6**	**92.7**	**92.6**	**0.04**	**0.18**	**0.09**
O6W3O1	**86.7**	**86.8**	**86.7**	**86.8**	**0.06**	**0.08**	**0.10**
O1W3O6	**78.0**	**77.9**	**78.0**	**77.8**	**0.16**	**0.08**	**0.21**
O6W3O6	**74.7**	**74.6**	**74.5**	**74.6**	**0.11**	**0.25**	**0.14**

All vibrational modes (Raman) of the samples and reference are shown in **Tab. S4**.

Table S4. Peak locations relative to the α-Ag_2WO_4 micro-Raman spectroscopy analysis.

	W	**WE0.25**	**WE0.5**	**Ref**
A_{1g}				**44**
A_{1g}				**60**
B_{1g}	**104**	**104**	**104**	**92**
A_{2g}				**116**
A_{2g}				**182**
A_{1g}		**206**		**208**
B_{1g}				**248**
A_{2g}	**308**	**308**	**308**	**306**
B_{2g}	**331**	**331**	**331**	**336**
A_{2g}	**380**	**380**	**380**	**366**
B_{2g}				**488**
B_{2g}	**500**	**500**		**510**

B_{2g}				**546**
A_{1g}	**575**	**575**		**590**
B_{1g}				**629**
B_{1g}	**660**	**660**	**660**	**667**
B_{1g}			**723**	**730**
B_{2g}	**731**	**731**	**731**	**754**
A_{1g}	**770**	**771**		**778**
A_{2g}				**800**
WO_4^{2-} (ν_3)			**828**	**832***
A_{1g}	**877**	**877**	**877**	**884**
WO_4^{2-} (ν_1)			**949**	**922***
References*[2, 4, *5]				

The literature shows that for different synthetic routes, without using surfactants or complexing agents, the α-Ag_2WO_4 shows a preferential formation of the eight-faceted hexagonal base rod-like morphology, which is composed by the (101), (010), and (001) surfaces, which are similar to those obtained by Cavalcante et al.[6] by the SC, CP, and CH methods, with only small modifications in the rod lengths. **Fig. S2** presents the TEM images of the particles obtained by the MAH method. **Fig. S2 (a-b)** show the microrods of the W sample. It can be observed that this sample displays (**Fig. S2(a)**) only some NPs on this surface, especially at the rods; however, this amount increases with the electron beam, as shown in **Fig. S2 (b)**. Although it is possible to have some NPs before the exposure to the electron microscope, they are mainly caused by the being exposed to the high-energy electron beam, as shown in **Fig. S2 (b)**. A few seconds after the beam in the TEM, it is possible to observe several filaments of metallic Ag, as reported by Longo et al.[7–12]. In **Fig. S2 (c-**

d), which refers to the WE0.25 sample, note the hollow structures consisting of nanorods and NPs. In this case, the NPs were already formed before the TEM analysis and they changed minimally with the increase in electron beam exposure time, as can be observed from the pictures in **Fig. S2 (c-d)**. Finally, note the flower-like structures consisting of microrods and NPs in the WE0.5 sample shown in **Fig. S2 (e-f)**. This sample was very unstable under the electron beam irradiation and the NPs on the surface started to grow, forming filaments by sintering and making the visualization of the planes of the NPs in the high-resolution TEM analysis difficult because the particles are constantly growing, as shown in **Fig. S3 (a-b)**. The differences of growth, shape, and stability are due to the morphologic aspects, as the NPs growth is a surface dependent property, as shown by Macedo et al.[13], comparing the differences of preferential Ag growth on two morphologies of α-Ag_2WO_4.

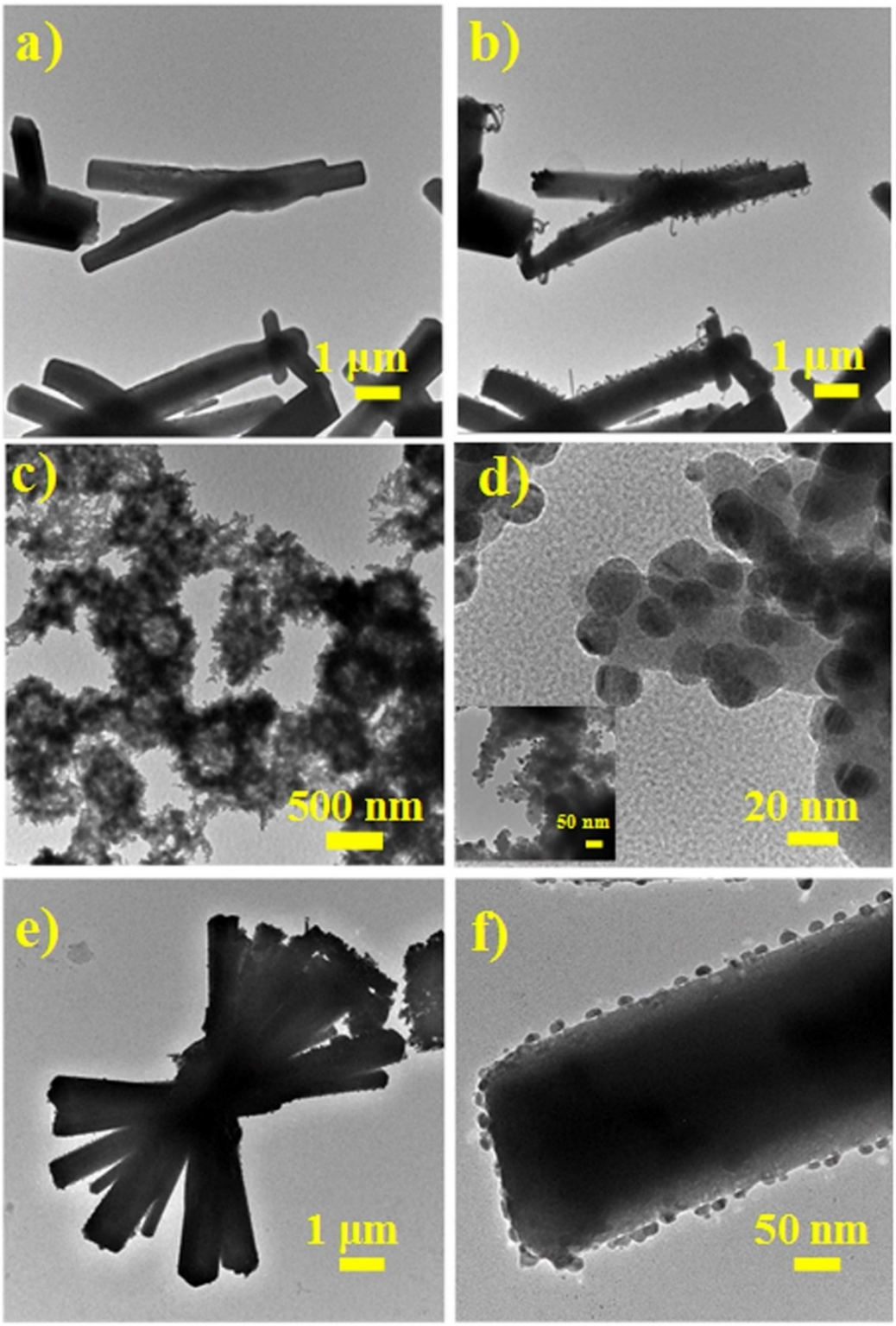

Figure S2. TEM images of samples exposed to a 200 kV electron beam. a, b) W; c, d) WE0.25 and e, f) WE0.5.

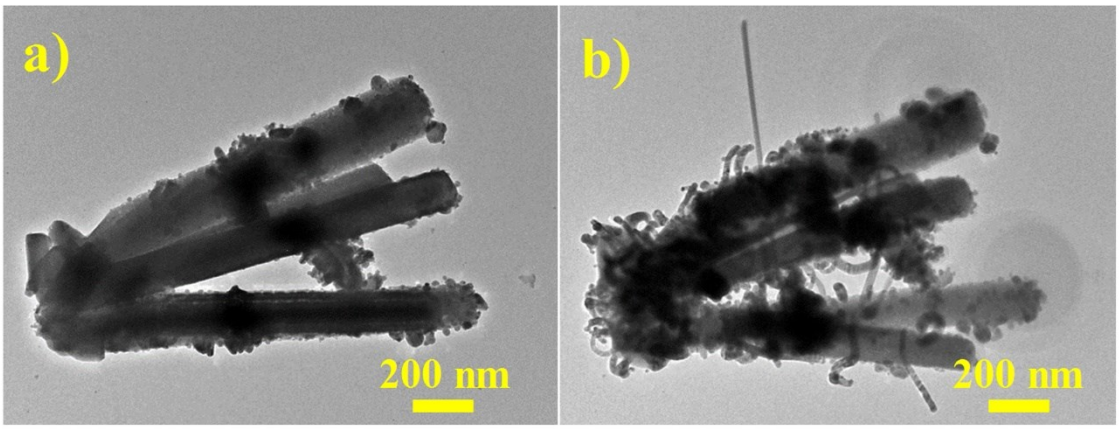

Figure S3. Low-resolution TEM analysis of the WE0.5 sample of the α-Ag_2WO_4 and Ag NPs at a) at time zero and b) 10 seconds later.

REFERENCES

1 P. M. Skarstad and S. Geller, *Mat. Res. Bull*, 1975, **10**, 791–799.

2 D. Stone, J. Liu, D. P. Singh, C. Muratore, A. A. Voevodin, S. Mishra, C. Rebholz, Q. Ge and S. M. Aouadi, *Scr. Mater.*, 2010, **62**, 735–738.

3 M. D. P. Silva, R. F. Gonçalves, I. C. Nogueira, V. M. Longo, L. Mondoni, M. G. Moron, Y. V Santana and E. Longo, *Spectrochim. Acta Part A Mol. Biomol. Spectrosc.*, 2016, **153**, 428–435.

4 A. Turkovic, L. Fox, J. F. Scott, S. Geller and G. F. Ruse, *Mat. Res. Bull*, 1977, **12**, 189–196.

5 H. Feilchenfeld and O. Siiman, *J. Phys. Chem.*, 1986, **90**, 4590–4599.

6 L. S. Cavalcante, M. A. P. Almeida, W. Avansi, R. L. Tranquilin, E. Longo, N. C. Batista, V. R. Mastelaro and M. S. Li, *Inorg. Chem.*, 2012, **51**, 10675–10687.

7 L. F. Da Silva, A. C. Catto, W. Avansi, A. Mesquita, L. J. Q. Maia, O. F. Lopes, M. S. Li, M. L. Moreira, E. Longo, J. Andrés and V. R. Mastelaro, *Phys. Chem. Chem. Phys.*, 2019, **21**, 22031–22038.

8 W. da S. Pereira, J. Andrés, L. Gracia, M. A. San-Miguel, E. Z. da Silva, E. Longo and V. M. Longo, *Phys. Chem. Chem. Phys.*, 2015, **17**, 5352–5359.

9 E. Longo, L. S. Cavalcante, D. P. Volanti, A. F. Gouveia, V. M. Longo, J. A. Varela, M. O. Orlandi and J. Andrés, *Sci. Rep.*, 2013, **3**, 4–7.

10 E. Longo, W. Avansi, J. Bettini, J. Andrés and L. Gracia, *Sci. Rep.*, 2016, **6**, 1–8.

11 E. Longo, D. P. Volanti, V. M. Longo, L. Gracia, I. C. Nogueira, M. A. P. Almeida, A. N. Pinheiro, M. M. Ferrer, L. S. Cavalcante and J. Andrés, *J. Phys. Chem. C*, 2014, **118**, 1229–1239.

12 V. M. Longo, C. C. De Foggi, M. M. Ferrer, A. F. Gouveia, R. S. André, W. Avansi, C. E. Vergani, A. L. Machado, J. Andrés, L. S. Cavalcante, A. C. Hernandes and E. Longo, *J. Phys. Chem. A*, 2014, **118**, 5769–5778.

13 N. G. Macedo, T. R. Machado, R. A. Roca, M. Assis, C. C. Foggi, V. Puerto-Belda, G. Mínguez-Vega, A. Rodrigues, M. A. San-Miguel, E. Cordoncillo, H. Beltrán-Mir, J. Andrés and E. Longo, *ACS Appl. Bio Mater.*, 2019, **2**, 824–837.